

Figure 1. X-ray diagram of fresh VMgO catalyst. Peaks of  $\alpha$ - $\text{Mg}_2\text{V}_2\text{O}_7$ ,  $\circ$   $\beta$ - $\text{MgV}_2\text{O}_6$

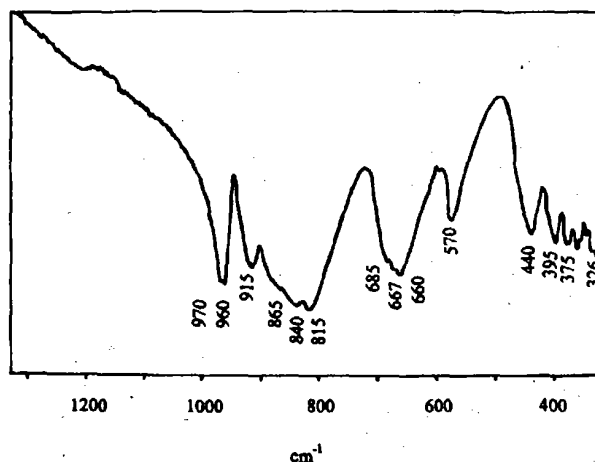


Figure 2. Infrared spectra of VMgO catalyst.

Nonlinear regression analysis was used to examine the fit of different kinetic models. For a given model, the reaction rate was integrated over the contact time, at each of the experimental conditions, to calculate the conversion predicted by the model. The Marquardt algorithm was used to search for the values of the model parameters that minimized the sum of the squared residuals.

## Results and Discussion

**Catalyst Characterization.** VMgO catalyst was obtained from MgO and  $\text{NH}_4\text{VO}_3$ . After calcination, the catalyst was of a pale yellow color. After use, it was

gray, which indicated the reduction of vanadium to an oxidation state lower than 5. The BET specific surface area was  $8.8 \text{ m}^2/\text{g}$ . Within the precision limit of the BET method no differences in surface area between fresh and used catalysts were detected. The X-ray diffraction pattern is shown in Figure 1. The spectrum revealed the dominant presence of  $\alpha$ - $\text{Mg}_2\text{V}_2\text{O}_7$  (ASTM file 31-816) with slight impurity of  $\beta$ - $\text{MgV}_2\text{O}_6$  in good agreement with that observed by Siew Hew Sam et al. (1990). The XRD analysis of used catalyst indicated that there were no detectable differences in the bulk structure after reaction; thus, the changes to the catalyst were limited to the surface. The infrared spectrum is presented in

Table 1. Experimental Results

| $Y_{\text{EtOH}}$<br>(mol %) | $Y_{\text{O}_2}$<br>(mol %) | $W/F$<br>( $\text{g h mol}^{-1}$ ) | $T$<br>(K) | $X$<br>(%)        | $Y_{\text{EtOH}}$<br>(mol %) | $Y_{\text{O}_2}$<br>(mol %) | $W/F$<br>( $\text{g h mol}^{-1}$ ) | $T$<br>(K) | $X$<br>(%) |
|------------------------------|-----------------------------|------------------------------------|------------|-------------------|------------------------------|-----------------------------|------------------------------------|------------|------------|
| 0.046                        | 0.059                       | 99.7                               | 453        | 4.8               | 0.084                        | 0.059                       | 52.6                               | 473        | 6.7        |
| 0.046                        | 0.059                       | 125                                | 453        | 5.1               | 0.084                        | 0.059                       | 77.5                               | 473        | 8.7        |
| 0.046                        | 0.059                       | 199.8                              | 453        | 7.5 <sup>a</sup>  | 0.084                        | 0.059                       | 105.2                              | 473        | 12.9       |
| 0.046                        | 0.059                       | 199.8                              | 453        | 7.5 <sup>a</sup>  | 0.084                        | 0.059                       | 172.6                              | 473        | 21.8       |
| 0.046                        | 0.059                       | 199.8                              | 453        | 7.5 <sup>a</sup>  | 0.084                        | 0.059                       | 52.6                               | 493        | 15.7       |
| 0.046                        | 0.059                       | 99.7                               | 473        | 12.3              | 0.084                        | 0.059                       | 77.5                               | 493        | 20.6       |
| 0.046                        | 0.059                       | 125                                | 473        | 13.7              | 0.084                        | 0.059                       | 105.2                              | 493        | 31.6       |
| 0.046                        | 0.059                       | 199.8                              | 473        | 21.2 <sup>a</sup> | 0.084                        | 0.059                       | 172.6                              | 493        | 45.7       |
| 0.046                        | 0.059                       | 199.8                              | 473        | 21 <sup>a</sup>   | 0.084                        | 0.059                       | 52.6                               | 513        | 36.3       |
| 0.046                        | 0.059                       | 199.8                              | 473        | 20.8 <sup>a</sup> | 0.084                        | 0.059                       | 77.5                               | 513        | 50         |
| 0.046                        | 0.059                       | 99.7                               | 493        | 25                | 0.084                        | 0.059                       | 105.2                              | 513        | 61.7       |
| 0.046                        | 0.059                       | 125                                | 493        | 30                | 0.084                        | 0.059                       | 172.6                              | 513        | 87         |
| 0.046                        | 0.059                       | 199.8                              | 493        | 48.5 <sup>a</sup> | 0.033                        | 0.09                        | 199.8                              | 453        | 8.1        |
| 0.046                        | 0.059                       | 199.8                              | 493        | 46 <sup>a</sup>   | 0.033                        | 0.09                        | 199.8                              | 473        | 22.4       |
| 0.046                        | 0.059                       | 199.8                              | 493        | 48.7 <sup>a</sup> | 0.033                        | 0.09                        | 199.8                              | 493        | 52.8       |
| 0.046                        | 0.059                       | 99.7                               | 513        | 55                | 0.033                        | 0.09                        | 199.8                              | 513        | 88.7       |
| 0.046                        | 0.059                       | 125                                | 513        | 65                | 0.046                        | 0.09                        | 199.8                              | 453        | 8.4        |
| 0.046                        | 0.059                       | 199.8                              | 513        | 84.6 <sup>a</sup> | 0.046                        | 0.09                        | 199.8                              | 473        | 21.7       |
| 0.046                        | 0.059                       | 199.8                              | 513        | 87.1 <sup>a</sup> | 0.046                        | 0.09                        | 199.8                              | 493        | 51.6       |
| 0.046                        | 0.059                       | 199.8                              | 513        | 85 <sup>a</sup>   | 0.046                        | 0.09                        | 199.8                              | 513        | 86.2       |
| 0.063                        | 0.059                       | 71.6                               | 453        | 3.8               | 0.057                        | 0.09                        | 199.8                              | 453        | 8.3        |
| 0.063                        | 0.059                       | 105.4                              | 453        | 4.5               | 0.057                        | 0.09                        | 199.8                              | 473        | 23.2       |
| 0.063                        | 0.059                       | 143.13                             | 453        | 5.5               | 0.057                        | 0.09                        | 199.8                              | 493        | 55         |
| 0.063                        | 0.059                       | 71.6                               | 473        | 8.8               | 0.057                        | 0.09                        | 199.8                              | 513        | 83.1       |
| 0.063                        | 0.059                       | 105.4                              | 473        | 12.7              | 0.046                        | 0.135                       | 199.8                              | 453        | 9.7        |
| 0.063                        | 0.059                       | 143.13                             | 473        | 14.6              | 0.046                        | 0.135                       | 199.8                              | 473        | 26.3       |
| 0.063                        | 0.059                       | 71.6                               | 493        | 22.3              | 0.046                        | 0.135                       | 199.8                              | 493        | 61         |
| 0.063                        | 0.059                       | 105.4                              | 493        | 29.8              | 0.046                        | 0.135                       | 199.8                              | 513        | 91.4       |
| 0.063                        | 0.059                       | 143.13                             | 493        | 36.3              | 0.046                        | 0.198                       | 199.8                              | 453        | 11.4       |
| 0.063                        | 0.059                       | 71.6                               | 513        | 42                | 0.046                        | 0.198                       | 199.8                              | 473        | 29.9       |
| 0.063                        | 0.059                       | 105.4                              | 513        | 59.6              | 0.046                        | 0.198                       | 199.8                              | 493        | 66.7       |
| 0.063                        | 0.059                       | 143.13                             | 513        | 74.9              | 0.046                        | 0.198                       | 199.8                              | 513        | 94.8       |
| 0.084                        | 0.059                       | 52.6                               | 453        | 2.9               | 0.063                        | 0.09                        | 180.6                              | 473        | 19.7       |
| 0.084                        | 0.059                       | 77.5                               | 453        | 3.3               | 0.063                        | 0.09                        | 180.6                              | 493        | 44         |
| 0.084                        | 0.059                       | 105.2                              | 453        | 3.8               | 0.084                        | 0.198                       | 172.6                              | 493        | 65.4       |
| 0.084                        | 0.059                       | 172.6                              | 453        | 9.2               | 0.084                        | 0.198                       | 172.6                              | 473        | 28.4       |

<sup>a</sup> Experimental set for diffusional control.

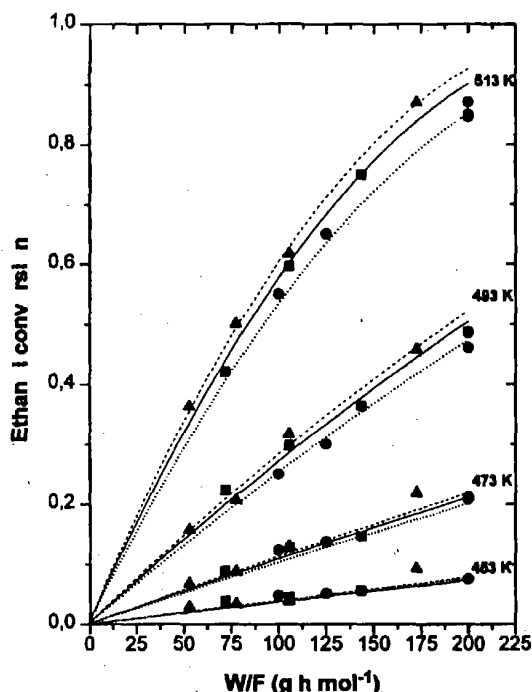


Figure 3. Ethanol conversion vs. space time at different inlet concentration of ethanol and temperatures. Curves: kinetic model, points: experimental data (partial pressure of oxygen = 41.3 mmHg). Key:  $\Delta$ , 8.4 mol % of ethanol;  $\blacksquare$ , 6.3 mol %;  $\bullet$ , 4.6 mol %.

Table 2. Selectivity to Acetaldehyde at 513 K<sup>a</sup>

| $Y_{\text{EtOH}}$ (mol %) | conversion (%) | selectivity to AcH (%) |
|---------------------------|----------------|------------------------|
| 0.046                     | 55.0           | 96.9                   |
| 0.046                     | 65.0           | 96.1                   |
| 0.046                     | 85.0           | 95.0                   |
| 0.063                     | 42.0           | 98.7                   |
| 0.063                     | 59.6           | 97.0                   |
| 0.063                     | 74.9           | 95.6                   |
| 0.084                     | 36.3           | 97.8                   |
| 0.084                     | 50.0           | 96.2                   |
| 0.084                     | 61.7           | 94.8                   |
| 0.084                     | 87.0           | 93.0                   |

<sup>a</sup> Partial pressure of oxygen: 41.3 mmHg.

Figure 2. The presence of pyrovanadate was revealed through its bands (326, 362, 395, 440, 570, 667, 685, 815, 915, 960, and 970  $\text{cm}^{-1}$ ) (Siew Hew Sam et al., 1990). The bands at 970 and 960  $\text{cm}^{-1}$  are attributed to a V=O bond characteristic of magnesium pyrovanadate. The IR spectrum confirms the X-ray diffraction.

**Catalytic Results.** The oxidation of ethanol over VMgO was carried out between 453 and 513 K. The experimental data are collected in Table 1. The main oxidation product was acetaldehyde with selectivity greater than 90%. At higher temperatures,  $\text{CO}_2$ , ethylene, and oxygenated products were obtained as minor products. The maximum in  $\text{CO}_2$  selectivity was around 6%.  $\text{CH}_4$ , CO, or acetic acid was not detected under the reaction conditions used. Thus, VMgO catalyst has a high selectivity to acetaldehyde at a temperature range lower than the industrial process (McKetta, 1988; Chauvel et al., 1986). The catalytic activity and the selectivity did not change after 12 h of reaction. No deactivation by coke formation or sintering was observed, and the catalyst can be reused without additional treatment.

Figure 3 illustrates the effect of W/F in ethanol conversion. These results reveal a weak influence of the inlet concentration of ethanol. As expected, the

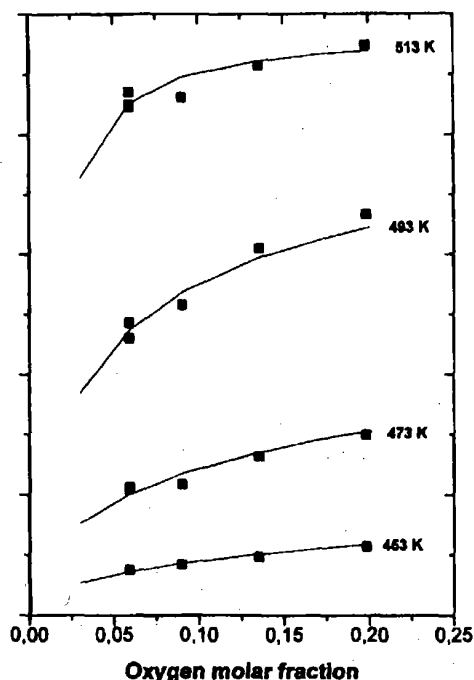


Figure 4. Ethanol conversion vs. molar fraction of oxygen. Curves: kinetic model. Points: experimental data (W/F = 199.8  $\text{g h mol}^{-1}$ , inlet concentration of ethanol = 4.6 mol %).

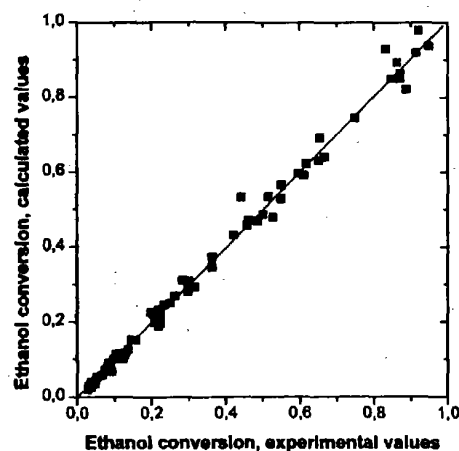


Figure 5. Parity plot for the conversion of ethanol.

Table 3. Estimation of Frequency Factors and Activation Energies from the Data at All Temperatures<sup>a</sup>

| param | estimated value                                   | $t_{\text{calcd}}$ | units   |
|-------|---|--------------------|---|
| $k_R$ | $k_R^*: 3.34 \times 10^6 \pm 8.1 \times 10^5$     | 82.5               | $\text{mol g}^{-1} \text{h}^{-1} \text{atm}^{-1}$   |
|       | $E_R: 16194 \pm 385$                              | 83.3               | cal/mol   |
| $k$   | $k^*: 8.39 \times 10^{-3} \pm 2.2 \times 10^{-4}$ | 76.6               | $\text{atm}^{-1/2}$                                 |
|       | $\Delta E: -7331 \pm 175$                         | 83.7               | cal/mol   |
| $k_O$ | $k_O^*: 3.985 \times 10^8$                        |                    | $\text{mol g}^{-1} \text{h}^{-1} \text{atm}^{-1/2}$ |
|       | $E_O: 23525$                                      |                    | cal/mol   |

<sup>a</sup> F value 3800. Correlation coefficient: 0.99. Confidence limits: 95%.

higher the temperature, the higher the conversion with only a small decrease in the selectivity, Table 2.

The dependence of conversion on oxygen partial pressure was also studied in a similar manner. Figure 4 shows the conversion versus the oxygen molar fraction. The higher the oxygen partial pressure, the higher the conversion. In all cases, the oxygen conversion was less than 100%.

Tabl

Cu  
Cc  
0.1  
1.1  
V<sub>2</sub>  
α-  
VI

R  
to a

C<sub>2</sub>H  
Cl

TI  
cata  
tem

f r  
initi

part  
Hew

und  
colo

usec  
(Ma

the  
cata

The  
site

oxid  
amo

ates  
reac

etha

r =

k =

av i

root

part

ads

(Gel

Th

the i

teste

data

all t

expo

illus

sion

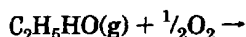
3 sh

t val

Table 4. Comparison with Previous Works on Different Catalysts

| catalyst   | activation energy (kcal/mol) | T range (K) | selectivity to acetaldehyde (%) |
|--|------------------------------|-------------|---------------------------------|
| Cu(II)NaY (Tsuruya et al., 1985)   | 16.9                         | 523–623     | 100                             |
| Co(II)NaY (Tsuruya et al., 1985)   | 15.5                         | 523–623     | 100                             |
| 0.5 wt % Cr/SiO <sub>2</sub> (Parlitz et al., 1985)  | 14.0                         | 513         | 39.8                            |
| 1.21 wt % Cr/SiO <sub>2</sub> (Parlitz et al., 1985)   | 17.5                         | 513         | 66.8                            |
| V <sub>2</sub> O <sub>5</sub> /α-Al <sub>2</sub> O <sub>3</sub> (Quaranta et al., 1993)      |                              | 520         | 100                             |
| α-Sb <sub>2</sub> O <sub>4</sub> -Fe(MoO <sub>4</sub> ) <sub>3</sub> (Castillo et al., 1993) |                              | 623         | 92                              |
| VMgO (present work)  | 16.2                         | 453–513     | 100–90                          |

**Reaction Kinetics.** Oxidehydrogenation of ethanol to acetaldehyde and water is an exothermic reaction.



The VMgO system was found to be an excellent catalyst to perform this reaction at relatively low temperature. In α-Mg<sub>2</sub>V<sub>2</sub>O<sub>7</sub>, the presence of two different bonds was found: a V=O short bond that could initiate an H abstraction and a V–O–V bond that could participate in the mechanism of water formation (Siew Hew Sam et al., 1990). During reaction, this catalyst undergoes a reduction–reoxidation cycle. A change in color from pale yellow to gray was observed after being used. A Mars–van Krevelen redox reaction mechanism (Mars and van Krevelen, 1954) can be assumed for the ethanol oxidation over VMgO catalysts. Two types of catalyst sites are considered: reduced and oxidized sites. The ethanol reacts on the oxidized site by reducing the site with a rate constant,  $k_R$ , and the reduced site is oxidized by oxygen with a rate constant,  $k_O$ . The amount of surface being covered by adsorbed intermediates is considered negligible. At steady state, the reaction rate defined as the rate of disappearance of ethanol is

$$r = k_R k_O P_E P_O^{1/2} / (k_R P_E + k_O P_O^{1/2}) = k_R P_E P_O^{1/2} / (k P_E + P_O^{1/2})$$

$k = k_R/k_O$  being a lumped parameter. This approach avoided an excessive correlation parameter. A square root dependence of the reaction rate on the oxygen partial pressure could be indicating that a dissociatively adsorbed oxygen is involved in the reoxidation step (Gellings and Bouwmeester, 1992).

The kinetic analysis of data was carried out by using the integral method. The adequacy of this model was tested by fitting the above equation to the experimental data. Parameter estimations per temperature and at all temperatures were carried out so as to obtain pre-exponential factors and activation energies. Figure 5 illustrates the parity plot of the overall ethanol conversion after estimation based on all temperatures. Table 3 shows the parameter estimates. The high  $F$  value and  $t$  values indicate the adequacy of the model and the significance of its parameters, respectively. From  $k_R$  and  $k$ , the activation energy and the frequency factor for the reoxidation were calculated, and they are also shown in Table 2. The activation energy of reaction,  $E_R = 16.2$  kcal/mol, is lower than that for reoxidation,  $E_O = 23.5$  kcal/mol, in agreement with literature (Creaser and Andersson, 1996). This indicates that the catalyst tends to be more oxidized at higher temperature, which corresponds to the higher oxidized site concentration. The activation energy for the reoxidation reaction is near the value found for reoxidation of vanadium in V<sub>2</sub>O<sub>5</sub> catalyst (Mars and van Krevelen, 1954).

With the parameter values, the conversion was calculated by means a numerical integration of the rate equation using a fourth-order Runge Kutta method. The fitting shown in Figures 3 and 4 is satisfactory.

In Table 4, a comparison with previous works on different catalytic systems is shown. VMgO catalyst has a similar activity with a high selectivity to acetaldehyde at lower temperature.

## Conclusions

From the results described above, VMgO was found to be a very active and selective oxidative dehydrogenation catalyst for ethanol. The selectivity to acetaldehyde was 100% up to 493 K, which is a temperature much lower than the one used in the industrial process. X-ray diffraction and infrared spectroscopy suggested that the active phase was magnesium pyrovanadate. The catalytic function for ethanol oxidation depends on the redox ability of vanadium to alternate between different valence states. A rate equation was developed on the basis of a steady-state redox model, and activation energies for the two partial steps were determined, which showed that the overall rate is most influenced by catalyst reoxidation. The Mars–van Krevelen mechanism was reasonable to explain the experimental results.

## Acknowledgment

The authors wish to thank Ing. Cadus L. for his help in preparing the catalyst and Dr. Pedregosa for performing the IR experiment. They also are indebted to Dr. Rivarola for his timely help in one way or another. The financial support of CONICET and Universidad Nacional de San Luis is gratefully acknowledged.

## Literature Cited

- Allakhverdova, N.; Adzhamov, K.; Alkhazov, T. Oxidation of ethanol to acetic acid over a tin–molybdenum oxide catalyst. *Kinet. Katal.* **1992a**, *33*(2), 261.
- Allakhverdova, N.; Kerimov, Kh.; Alkhazov, T. Oxidation of ethanol on a cerium-promoted Sn–Mo oxide catalyst. *Kinet. Katal.* **1992b**, *33*(3), 473.
- Bagiev, V.; Dadashev, G.; Adzhamov, K.; Alkhazov, T. Hetero-homogenic conversions of ethanol on Sn–Mo oxide catalyst. *Kinet. Katal.* **1992**, *33*(3), 460.
- Carrazan, S.; Peres, C.; Bernard, J.; Ruwet, M.; Ruiz, P.; Delmon, B. Catalytic Synergy in the oxidative dehydrogenation of propane over MgVO Catalysts. *J. Catal.* **1996**, *158*, 452.
- Castillo, R.; Awasarkar, P. A.; Papadopolou, Ch.; Acosta, D.; Ruiz, P. Creation of new selective sites by spillover oxygen in the oxidation of ethanol. II World Congress & IV European Workshop Meeting. *New Developments in Selective Oxidation*, Benalmadena, Spain, Cortes Corberan, V., Vic Bellon, S., Eds.; 1993; p 13–1.
- Chaar, M. A.; Patel, D.; Kung, M. C.; Kung, H. H. Selective oxidative Dehydrogenation of butane over V–Mg–O catalysts. *J. Catal.* **1987**, *105*, 483.
- Chaar, M. A.; Patel, D.; Kung, H. H. Selective Oxidative Dehydrogenation of propane over V–Mg–O Catalysts. *J. Catal.* **1988**, *109*, 463.

- Chauvel, A.; Lefebvre, G.; Castex, L. *Procedes de petrochimie—Caracteristiques techniques et economiques*; Ed. Technip: Paris, 1986; tome 2, p 33.
- Corma, A.; Lopez Nieto, J. M.; Parede, N. Influence of the preparation methods of V-Mg-O catalysts on their catalytic properties for the oxidative dehydrogenation of propane. *J. Catal.* **1993**, *144*, 425.
- Creaser, D.; Andersson, B. Oxidative dehydrogenation of propane over VMgO: Kinetic investigation by nonlinear regression analysis. *Appl. Catal. A: Gen.* **1996**, *141*, 131.
- Gellings, P. J.; Bouwmeester H. J. M. Ion and mixed conducting oxides as catalysts. *Catal. Today* **1992**, *12*, 65.
- Ling, T. R.; Chem, Z.-B.; Lee, M.-D. Catalytic behavior and electrical conductivity of LaNiO<sub>3</sub> in Ethanol Oxidation. *Appl. Catal. A: Gen.* **1996**, *136*, 191.
- Mamedov, E. A.; Cortes Corberan, V. Oxidative dehydrogenation of lower alkanes on vanadium oxide-based catalysts. The present state of the art and outlooks. *Appl. Catal. A: Gen.* **1995**, *127*, 1.
- Mars, P.; van Krevelen, D. W. Oxidations carried out by means of vanadium oxide catalysts. *Chem. Eng. Sci. Special Suppl.* **1954**, *3*, 41.
- McKetta, J. J. *Encyclopedia of Chemical Processing and Design*; Marcel Dekker, Inc.: New York, 1988; vol 1, p 114.
- Parlitz, B.; Hanke, W.; Fricke, R.; Richter, M.; Roost, U.; Ohlmann, G. Studies on catalytically active surface compounds. XV. The catalytic oxidation of ethanol on Cr/SiO<sub>2</sub> catalysts and some relations to the structure. *J. Catal.* **1985**, *94*, 24.
- Quaranta, N. E.; Martino, R.; Gambaro, L.; Thomas, H. Selective Dehydrogenation of Ethanol over Vanadium Oxide Catalyst. II World Congress & IV European Workshop Meeting. *New Developments in Selective Oxidation*; Benalmadena, Spain; Cortes Corberan, V., Vic Bellon, S., Eds.; 1993; p 15-1.
- Siew Hew Sam, D.; Soenen, V.; Volta, J. C. Oxidative dehydrogenation of propane over V-Mg-O catalysts. *J. Catal.* **1990**, *123*, 417.
- Tsuruya, S.; Tsukamoto, M.; Watanabe, M.; Masai, M. Ethanol oxidation over Y-type zeolite ion-exchanged with copper(II) and cobalt(II) ions. *J. Catal.* **1985**, *93*, 303.

Received for review January 10, 1997

Revised manuscript received May 27, 1997

Accepted May 27, 1997\*

IE970040K

\* Abstract published in *Advance ACS Abstracts*, July 15, 1997.

Ir

1.

to  
ca  
ac  
in  
ze  
M  
al  
so  
tic  
m  
t  
(N  
x  
ch

th  
se  
f  
ie  
ar  
in  
st  
pr  
fo  
ti  
th  
f  
al  
ba  
st  
th  
m  
ve  
ti

is